Frontiers in Earth Science

TYPE Original Research
PUBLISHED 24 February 2023
DOI 10.3389/feart.2023.1084399

Quantifying the contributions of climate factors and human activities to variations of net primary productivity in China from 2000 to 2020

Zijian Li[1], Jiangping Chen[1,2]*, Zhanpeng Chen[3]*, Zongyao Sha[1,4], Jianhua Yin[1] and Zhaotong Chen[1]

[1]School of Remote Sensing and Information Engineering, Wuhan University, Wuhan, China, [2]Key Laboratory of National Geographical Census and Monitoring, Ministry of Natural Resources, Wuhan, China, [3]Institute of Land Resources Surveying and Mapping of Guangdong Province, Guangzhou, China, [4]Key Laboratory of Natural Resources Monitoring in Tropical and Subtropical Area of South China, Ministry of Natural Resources, Guangzhou, China

Net primary productivity (NPP) plays a vital role in the globe carbon cycle. Quantitative assessment of the effects of climate changes and human activities on net primary productivity dynamics is vital for understanding the driving mechanisms of vegetation change and sustainable development of ecosystems. This study investigates the contributions of climatic factors and human activities to vegetation productivity changes in China from 2000 to 2020 based on the residual trend analysis (RESTREND) method. The results showed that the annual average net primary productivity in China was 325.11 g C/m^2/year from 2000 to 2020 and net primary productivity showed a significantly increasing trend ($p<0.05$) at a rate of 2.32 g C/m^2/year. Net primary productivity increased significantly ($p<0.05$) across 40.90% of China over the study period, while only 1.79% showed a significantly declining trend ($p<0.05$). The contributions of climatic factors and human activities to net primary productivity increase were 1.169 g C/m^2/year and 1.142 g C/m^2/year, respectively. Climate factors contributed positively mainly in Sichuan Basin, the Loess Plateau, the Mongolian Plateau, and Northeast China Plain. Positive contributions of human activities to net primary productivity mainly occurred in the Loess Plateau, Central China, and the Greater Khingan Mountains. The effects of climatic factors and human activities on net primary productivity changes varied among sub-regions. In Tropical Monsoon Climate Region and Subtropical Monsoon Climate Region, human activities had greater impacts on net primary productivity increase than climate factors, while climate factors were the dominant factor for net primary productivity recovery in other sub-regions. In addition, during 2000–2020, net primary productivity was dominated by both climate factors and human activities in 49.84% of China, while areas dominated solely by climate factors and human activities accounted for 13.67% and 10.92%, respectively. Compared to changed land cover types, the total net primary productivity as well as the increase of total net primary productivity in China was mostly contributed by unchanged land cover types, which contributed more than 90%.

OPEN ACCESS

EDITED BY
Manoj Kumar,
Forest Research Institute (FRI), India

REVIEWED BY
Xuguang Tang,
Southwest University, China
Xiangjin Shen,
Northeast Institute of Geography and Agroecology (CAS), China
Dehua Mao,
Northeast Institute of Geography and Agroecology (CAS), China
Keshav Tyagi,
Forest Research Institute (FRI), India
Agnish Kumar Das,
Forest Research Institute (FRI), India

*CORRESPONDENCE
Jiangping Chen,
chen_jp@whu.edu.cn
Zhanpeng Chen,
chyczp1441@163.com

SPECIALTY SECTION
This article was submitted to Environmental Informatics and Remote Sensing,
a section of the journal
Frontiers in Earth Science

RECEIVED 30 October 2022
ACCEPTED 14 February 2023
PUBLISHED 24 February 2023

CITATION
Li Z, Chen J, Chen Z, Sha Z, Yin J and Chen Z (2023), Quantifying the contributions of climate factors and human activities to variations of net primary productivity in China from 2000 to 2020.
Front. Earth Sci. 11:1084399.
doi: 10.3389/feart.2023.1084399

KEYWORDS

net primary productivity (NPP), climate factors, human activities, residual trend analysis, China

1 Introduction

Net primary productivity (NPP) is the remainder of the total amount of organic matter produced by green plants per unit area per unit time, excluding that consumed by their own respiration (Roxburgh et al., 2005). NPP is an important indicator of regional ecosystem function, ecosystem stability and self-healing capacity (Melillo et al., 1993; Running et al., 2004). It is not only an important component of the global carbon cycle (Cramer et al., 1999; Crabtree et al., 2009), but also reflects the combined effects of climate changes and human activities on terrestrial vegetation (Gower et al., 1999; Nemani et al., 2003). Therefore, the analysis of the spatiotemporal evolution patterns and driving factors of vegetation NPP can provide a scientific basis for evaluating the quality of regional terrestrial ecosystems, effective management of natural resources, and sustainable socioeconomic development in the context of global climate change (Qi et al., 2019).

The driving factors of NPP changes can be divided into climate changes and human activities (Chen et al., 2014; Sun et al., 2015). It is believed that increased CO_2 fertilization effects in climate enhance vegetation NPP (Piao et al., 2011; Wang et al., 2020), which contributes a negative feedback effect on global warming. Regional temperature, precipitation and solar radiation are the most important climate factors driving NPP changes (Churkina and Running, 1998; Nemani et al., 2003; Running et al., 2004). Temperature, in high latitudes and altitudes, e.g., northeastern China (Li H. et al., 2021) and the Qinghai-Tibet Plateau (Xu et al., 2016; Wang S. et al., 2017), exerts the key climatic driver for NPP increases. The increase in temperature at cold regions can enhance activities of photosynthetic enzymes, reduce speed of chlorophyll degradation, and prolong the vegetation growth season, thus promote vegetation productivity (Liu et al., 2016; Dusenge et al., 2019). In arid and semi-arid areas, precipitation plays a decisive role in the NPP dynamics among the climatic factors, and the increase of precipitation enhances vegetation photosynthesis by affecting soil water content (Wang et al., 2001; Jiang Y. et al., 2020; Li C. et al., 2021). Solar radiation can influence soil temperature, and its increase reduces soil moisture and hinders root growth, thus decreasing productivity especially in low-land grassland ecosystems (Zhou et al., 2012; Wu G. et al., 2021). However, previous studies have also found that excessive solar radiation exerted a negative effect on vegetation productivity in the Qinghai-Tibet Plateau (Luo et al., 2018; Yan et al., 2019).

In addition, anthropogenic factors are also important drivers of vegetation dynamic. In order to improve the environment, the Chinese government has launched a variety of initiatives, including Three-North Shelter Forest Program, Grain to Green Program (GTGP), and Grazing Withdrawal Program (GWP) (Wang B. et al., 2017; Li et al., 2021a). The Loess Plateau, one of the world's most eroded regions, is a prioritized pilot region of the ongoing GTGP program and has shifted from a net carbon source to a net carbon sink by converting cultivated land on steep slopes to perennial vegetation (Feng et al., 2013; Gang et al., 2018). Decreased grazing pressure and conversion from grazing lands to grasslands resulting from these programs have made a significant contribution to vegetation restoration, and have greatly improved the carbon storage in the Qinghai-Tibet Plateau, and Inner Mongolia Grassland (Chi et al., 2018; Li et al., 2021b). In order to prevent and control rocky desertification issues in southwestern China, a series of key national ecological restoration projects such as the Natural Forest Protection Project and the Karst Rocky Desertification Comprehensive Control and Restoration Project have been launched and the world's leading level of vegetation productivity restoration have been achieved (Gang et al., 2019; Tang et al., 2022). China's climate is complex and diverse with an abundant number of ecosystems, spanning from south to north across tropical zone to cold temperate zone, and from the humid zone in the southeast to the arid zone in the northwest (Yang et al., 2017; Lai et al., 2018). However, effects of climate factors and human activities vary across climate zones and ecosystem types due to the interaction of complex geographic topography and climate change (Zhao et al., 2018; Chen Y. et al., 2019). Relatively few studies have been concerned with such differences due to climatic zones. Therefore, it is necessary to assess the relative roles of climate changes and human activities in vegetation dynamics quantitatively under different climatic zones, for an in-depth understanding of the mechanisms driving vegetation change.

Recently, several methods have been adopted to determine the interaction of climate factors and human activities on vegetation dynamics, such as the regression model method, redundancy analysis, and the Miami memorial model (Li D. et al., 2018; Wu N. et al., 2021; Xiong et al., 2021). The regression model method is the simplest, but it is hard to describe the complex interactions between vegetation and climatic factors, between that and human activities (Turner and Carpenter, 2017; Liu et al., 2020), and independent variable factors are difficult to quantify spatially, lead to uncertainties in the results (Wu N. et al., 2021). The biophysical model-based method can separate the relative contributions of climate change and human activities on vegetation dynamics by simulating potential NPP (PNPP) and actual NPP (ANPP) (Li et al., 2016; Li C. et al., 2021), but it needs lots of physiological and ecological parameters, which may cause the uncertainties of the model (Zhou et al., 2015). The residual trend analysis method (RESTREND) (Evans and Geerken, 2004) is a simple calculation that can separate spatially the impact of human activities on vegetation from the impact of climate changes using the residue of multiple regression between climate factors and vegetation indicators to quantify the extent of human activities (Wu et al., 2022; Yin et al., 2022). The disadvantage of method is that model calibration in the year assuming without human interference would introduce errors into the model itself (Jiang H. et al., 2020). Understanding the influence mechanisms of NPP is essential to providing targeted guidance for constructing ecological restoration programs.

Previous studies focus on a specific or local region, and there are fewer studies on the entire China, as a decisive region in the global carbon cycle. Accordingly, the objectives of this study were to 1) analyze the spatial distribution and temporal dynamic

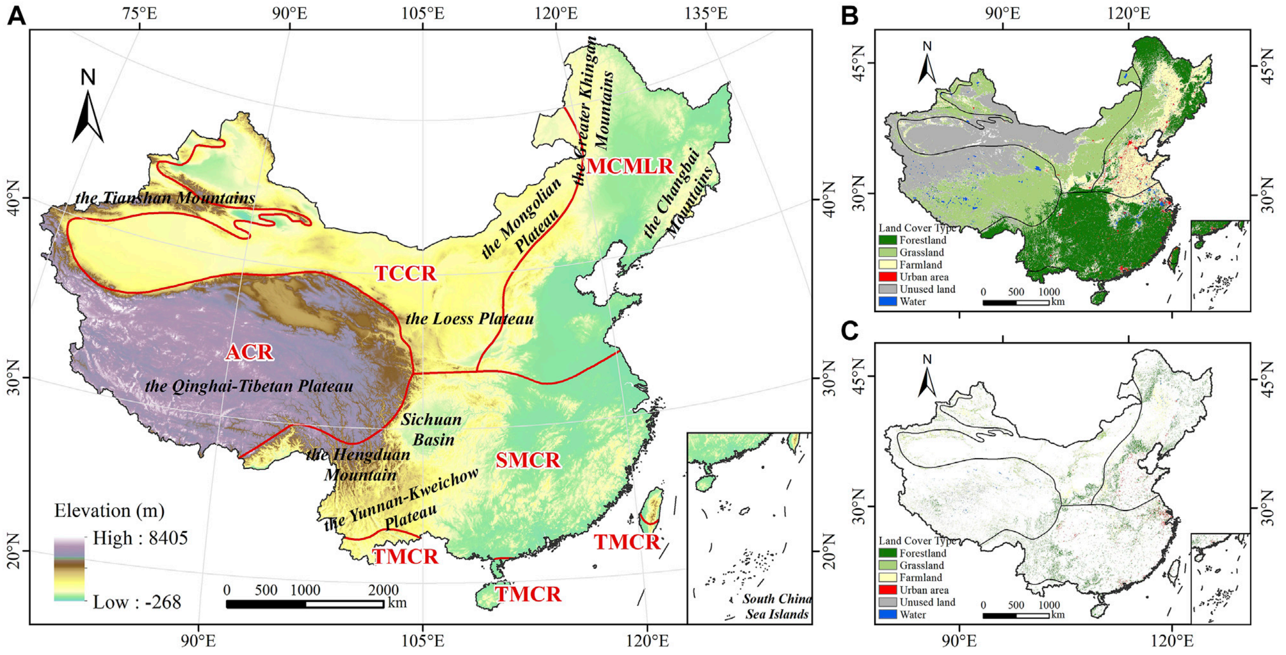

FIGURE 1
(A) The spatial pattern of elevation, the location of five sub-regions, and the distribution of **(B)** unchanged and **(C)** changed land cover types from 2001 to 2020. The legend of **(B)** means that the land cover type in 2020 was the same as that in 2001. The legend of **(C)** means the land cover type after conversion.

characteristics of NPP in China from 2000 to 2020; 2) quantify the contributions of climate factors and human activities to NPP dynamics in China; 3) explore the major driving factors of NPP changes under different climate types; 4) analyze the NPP dynamics for different land cover types.

2 Materials and methods

2.1 Study area and data

China, the third largest country in the world, was chosen as the study region, which had a complex topography, diverse climate, and rich variety of vegetation with an intricate distribution. China spanned a wide range of latitudes, with large differences in distance from the sea, as well as different terrain, resulting in diverse combinations of temperature and precipitation, forming a wide variety of climates. The local vegetation growth was significantly impacted by various climate types, thus we divided China into five regions (Figure 1) based on climate type for a more specific analysis (Song et al., 2011): 1) Tropical Monsoon Climate Region (TMCR); 2) Subtropical Monsoon Climate Region (SMCR); 3) Monsoon Climate Region of Medium Latitudes (MCMLR); 4) Temperate Continental Climate Region (TCCR); 5) Alpine Climate Region (ACR). During the growing season (from April to October), the average temperature differences across the country were not significant (except for ACR) with 24.4, 21.2, 16.2, 17.3, and 4.3°C. The cumulative precipitation rose from the northwest (170 mm) to the southeast (1,465 mm). On the contrary, the cumulative solar radiation increased from the southeast (3,702 MJ/m^2) to the northwest (5,161 MJ/m^2).

NPP data were derived from the Moderate Resolution Imaging Spectroradiometer (MODIS) Net Primary Production Gap-Filled Yearly L4 Global 500 m SIN Grid (MOD17A3HGF v006) from the National Aeronautics and Space Administration (NASA) (https://lpdaac.usgs.gov/) with a temporal resolution of 1 year and a spatial resolution of 500 m. The data were calculated by using an NPP estimation model established based on the Biome Biogeochemical model and the light use efficiency model. The downloaded NPP data from 2000 to 2020 were mosaiced, uniformly projected in WGS_1984_UTM_Zone_48N, converted to real values, and resampled to 1,000 m.

Monthly meteorological data of the growing season (from April to October) from 2000 to 2020 consisted of temperature, precipitation, and solar radiation. Temperature and precipitation data were obtained from the National Tibetan Plateau Data Center (https://data.tpdc.ac.cn/zh-hans/) with a spatial resolution of 1,000 m, which were generated by using Delta downscaling method based on the global climate dataset published by CRU and WorldClim. Solar radiation data were obtained from the National Centers for Environmental Prediction (NCEP) Climate Forecast System (CFS) (https://cfs.ncep.noaa.gov/) with a spatial resolution of 0.2°, and NCEP upgraded CFS to version 2 (CFSv2) on 30 March 2011. Data were resampled to 1,000 m. In this study, we defined the growing season as from April to October in order to be consistent across the whole country (Piao et al., 2010; Peng et al., 2011). The average temperature, the cumulative precipitation, and the cumulative solar radiation during the growing season from 2000 to 2020 were calculated.

Land cover data were downloaded from MODIS Land Cover Type Yearly L3 Global 500 m SIN Grid (MCD12Q1 v006) (https://

lpdaac.usgs.gov/) for the uniformity of data sources, and were resampled to 1,000 m. MODIS land cover types have been provided since 2001, thus data for 2001 and 2020 were used. Annual Plant Functional Types classification of MCD12Q1 was used for this study. In this study, we first analyzed NPP variations of the entire China and then areas of unchanged land cover types, as the area of changed land cover types accounted for only 7.29% of China, and the distribution was scattered (Figure 1).

Socio-economic data including gross domestic product (GDP) and population were obtained from the China Statistical Yearbooks (various issues) of the National Bureau of Statistics of China (http://www.stats.gov.cn/). Climate type distribution data were obtained from the Resources and Environment Science and Data Center, Chinese Academy of Sciences (http://www.resdc.cn/).

2.2 Methods

2.2.1 Trend analysis

The Theil-Sen trend analysis method was used to estimate the NPP change trend (Xu et al., 2020). The formula is as follows:

$$S_{NPP} = median\left[\frac{NPP_j - NPP_i}{j-i}\right], \forall i < j \tag{1}$$

Where S_{NPP} is the Theil-Sen trend of NPP and NPP_i and NPP_j are the values of NPP in year i and j, respectively. $S_{NPP} > 0$ indicates an increasing trend, and the converse denotes a decreasing trend.

The Mann-Kendall (MK) test was used to indicate the significance of the NPP trend (Dameneh et al., 2021). The formula is as follows:

$$S = \sum_{i=1}^{n-1}\sum_{j=i+1}^{n} sgn\left(NPP_j - NPP_i\right) \tag{2}$$

$$sgn\left(NPP_j - NPP_i\right) = \begin{cases} +1, NPP_j - NPP_i > 0 \\ 0, NPP_j - NPP_i = 0 \\ -1, NPP_j - NPP_i < 0 \end{cases} \tag{3}$$

$$Z = \begin{cases} \frac{S-1}{\sqrt{Var(S)}}, S > 0 \\ 0, S = 0 \\ \frac{S+1}{\sqrt{Var(S)}}, S < 0 \end{cases} \tag{4}$$

$$Var(S) = \frac{n(n-1)(2n+5)}{18} \tag{5}$$

Where n is the duration, in years, of the study period (n =21). When $|Z| > Z_{1-\alpha/2}$, the NPP trend is considered statistically significant. The 5% significant level which refers to $Z_{1-\alpha/2}$ =1.96 was used for the MK test in this study.

2.2.2 Contributions of climate factors and human activities to NPP

The main drivers of NPP changes are climate changes and human activities. The residual trend analysis (RESTREND) was used to calculate the contributions of climate factors (temperature, precipitation, and solar radiation) and human activities to NPP (Evans and Geerken, 2004). The formula is as follows:

$$S_{NPP} = C(C) + UF = C(T) + C(P) + C(R) + UF$$
$$\approx \left(\frac{\partial NPP}{\partial T}\right) \times \left(\frac{\partial T}{\partial n}\right) + \left(\frac{\partial NPP}{\partial P}\right) \times \left(\frac{\partial P}{\partial n}\right) + \left(\frac{\partial NPP}{\partial R}\right) \times \left(\frac{\partial R}{\partial n}\right) + C(H) \tag{7}$$

Where S_{NPP} is the Theil-Sen trend of NPP. $C(C), C(T), C(P), C(R)$ are the contributions of climate, temperature, precipitation, and solar radiation to NPP, respectively. $C(C)$ is the sum of $C(T), C(P)$, and $C(R)$. n is the number of study years. $C(T)$ is the product of $\partial NPP/\partial T$ (the slope of the linear regression line between NPP and temperature) and $\partial T/\partial n$ (the slope of the linear regression line between temperature; n). $C(P)$ and $C(R)$ are calculated similarly. In this study, the average temperature, the cumulative precipitation, and the cumulative solar radiation during the growing season (from April to October) were calculated. UF is residual value between S_{NPP}; $C(C)$. In this study; UF is interpreted as the change rate of the contribution of human activities to NPP, namely; $C(H)$ (Chen et al., 2021a; Ge et al., 2021).

2.2.3 Scenario design and quantitative evaluation methods

By combining the NPP trend with the contributions of the driving factors, six scenarios were produced according to the different permutations of value ranges of S_{NPP}, $C(C)$, and $C(H)$ (Table 1). Increased NPP is considered as an indicator of vegetation recovery, whereas a negative S_{NPP} stands for vegetation degradation (Zhou et al., 2015; Chen et al., 2021b). Positive $C(C)$ and $C(H)$ represent that climate factors and human activities facilitated an increase in NPP, whereas the negative $C(C)$ and $C(H)$ represent that climate factors and human activities caused a decline in NPP.

3 Results

3.1 Spatial and temporal variation of NPP

Figure 2A shows the spatial distribution of NPP from 2000 to 2020. In China, the annual average NPP ranged from 0 g C/m^2/year to 1943.59 g C/m^2/year and the average NPP in the region was 325.11 g C/m^2/year. The distribution pattern of NPP in China was higher in southeast and lower in northwest. TMCR had the highest NPP among the five sub-regions, with the average NPP of 1,110.11 g C/m^2/year. The average NPP in SMCR, MCMLR, and TCCR were 700.64 g C/m^2/year, 385.21 g C/m^2/year, and 105.41 g C/m^2/year, respectively. ACR had the lowest average NPP of 102.88 g C/m^2/year. As shown in Figure 2B, NPP increased in most of China in 2020 compared to 2000. NPP increased most significantly in the northeastern mountainous areas, the southern Loess Plateau, and Sichuan basin, with an increase of NPP of more than 200 g C/m^2/year. It can be seen that the NPP values in the southern Qinghai-Tibetan Plateau, the southern Yunnan-Kweichow Plateau, and the northern Greater Khingan Mountains were obviously reduced, with a decrease of NPP of more than 100 g C/m^2/year.

The annual NPP variations from 2000 to 2020 in China and five sub-regions were shown in Figure 2C. The annual average NPP in China showed a significantly increasing trend (p<0.05) at a rate of

TABLE 1 Six scenarios of NPP changes influenced by climate factors and human activities.

S_{NPP}	$C(C)$	$C(H)$	Contribution		Scenario
			Climate (%)	Human (%)	
>0	>0	>0	$\frac{\lvert C(C)\rvert}{\lvert C(C)\rvert+\lvert C(H)\rvert} \times 100$	$\frac{\lvert C(H)\rvert}{\lvert C(C)\rvert+\lvert C(H)\rvert} \times 100$	Recovery for both factors
	>0	<0	100	0	Recovery for climate factors
	<0	>0	0	100	Recovery for human activities
<0	<0	<0	$\frac{\lvert C(C)\rvert}{\lvert C(C)\rvert+\lvert C(H)\rvert} \times 100$	$\frac{\lvert C(H)\rvert}{\lvert C(C)\rvert+\lvert C(H)\rvert} \times 100$	Degradation for both factors
	<0	>0	100	0	Degradation for climate factors
	>0	<0	0	100	Degradation for human activities

TABLE 2 The contribution ratios of climate factors and human activities to NPP trend across China and five sub-regions.

Contribution ratio (%)	NPP variation		NPP recovery		NPP degradation	
	Climate	Human	Climate	Human	Climate	Human
China	50.58	49.42	50.25	49.75	47.58	52.42
TMCR	34.30	65.70	73.29	26.71	45.29	54.71
SMCR	40.79	59.21	42.58	57.42	48.85	51.15
MCMLR	53.84	46.16	53.31	46.69	24.70	75.30
TCCR	50.80	49.20	50.80	49.20	50.48	49.52
ACR	72.28	27.72	71.11	28.89	57.17	42.83

2.32 g C/m^2/year. In TMCR, NPP declined insignificantly ($p>0.05$) at a rate of −0.61 g C/m^2/year. However, NPP in the other four sub-regions showed a significant increasing trend ($p<0.05$). The increasing rate in MCMLR was highest, which was 4.44 g C/m^2/year, while NPP in ACR showed the lowest increasing rate of 0.62 g C/m^2/year. The increasing rate of SMCR and TCCR was 2.92 g C/m^2/year and 2.11 g C/m^2/year, respectively.

The spatial variations of NPP were observed, as shown in Figure 3. The classification in the legend of Figure 3A was determined by the distribution of NPP trend values, which between −5 and 10 accounted for 95% of the pixels. The NPP change trend in China ranged from −81.71 g C/m^2/year to 81.71 g C/m^2/year. NPP increased in 64.54% of China and 40.90% of the area increased significantly ($p<0.05$). The areas with rapid NPP increase were mainly distributed in Sichuan Basin, the Loess Plateau, and the Greater Khingan Mountains. In contrast, the decreasing trend of NPP accounted for 9.90% and 1.79% of the area declined significantly. The areas with NPP decrease mainly appeared in the southern Qinghai-Tibetan Plateau, the southern Yunnan-Kweichow Plateau, and southeastern China. Figure 3C shows the percentage changes of NPP for different regions. Areas of significant increases of NPP in TMCR, SMCR, MCMLR, TCCR, and ACR accounted for 23.55%, 43.77%, 67.20%, 37.17%, and 24.20%, respectively. NPP showed a significant decreasing trend across 19.33% of TMCR, 4.96% of SMCR, 0.61% of MCMLR, 0.15% of TCCR, and 0.45% of ACR, respectively.

3.2 Contributions of climate factors and human activities to NPP

The contributions of climate factors and human activities to NPP changes were calculated based on RESTREND (Figure 4). In China, the average contributions due to temperature, precipitation, and solar radiation to NPP were 0.205 g C/m^2/year, 0.467 g C/m^2/year, and 0.496 g C/m^2/year, respectively (Figure 4F). Besides, the contributions of climate and human activities were 1.169 g C/m^2/year and 1.142 g C/m^2/year. $C(C)$ of TMCR, SMCR, MCMLR, TCCR, and ACR were 0.482 g C/m^2/year, 1.225 g C/m^2/year, 2.312 g C/m^2/year, 1.066 g C/m^2/year, and 0.452 g C/m^2/year, respectively. However, human activities negatively contributed to NPP changes in TMCR, with the contribution of −0.924 g C/m^2/year. In contrast, $C(H)$ of SMCR, MCMLR, TCCR, and ACR were 1.778 g C/m^2/year, 1.982 g C/m^2/year, 1.033 g C/m^2/year, and 0.173 g C/m^2/year, respectively, having positive contributions to increases of NPP. Specific to each region, human activities played a primary role in NPP dynamics in TMCR and SMCR, whereas climate change was the dominant factor in the remaining regions, namely, MCMLR, TCCR, and ACR.

As shown in Figure 4A, temperature contributed positively in 46.27% of the area of China mainly including the Qinghai-Tibetan Plateau, the Loess Plateau, the Yunnan-Kweichow Plateau, and northeastern China, while temperature contributed negatively in 28.21% of China mainly including the Mongolian Plateau, eastern and southern China. Areas with positive contributions of

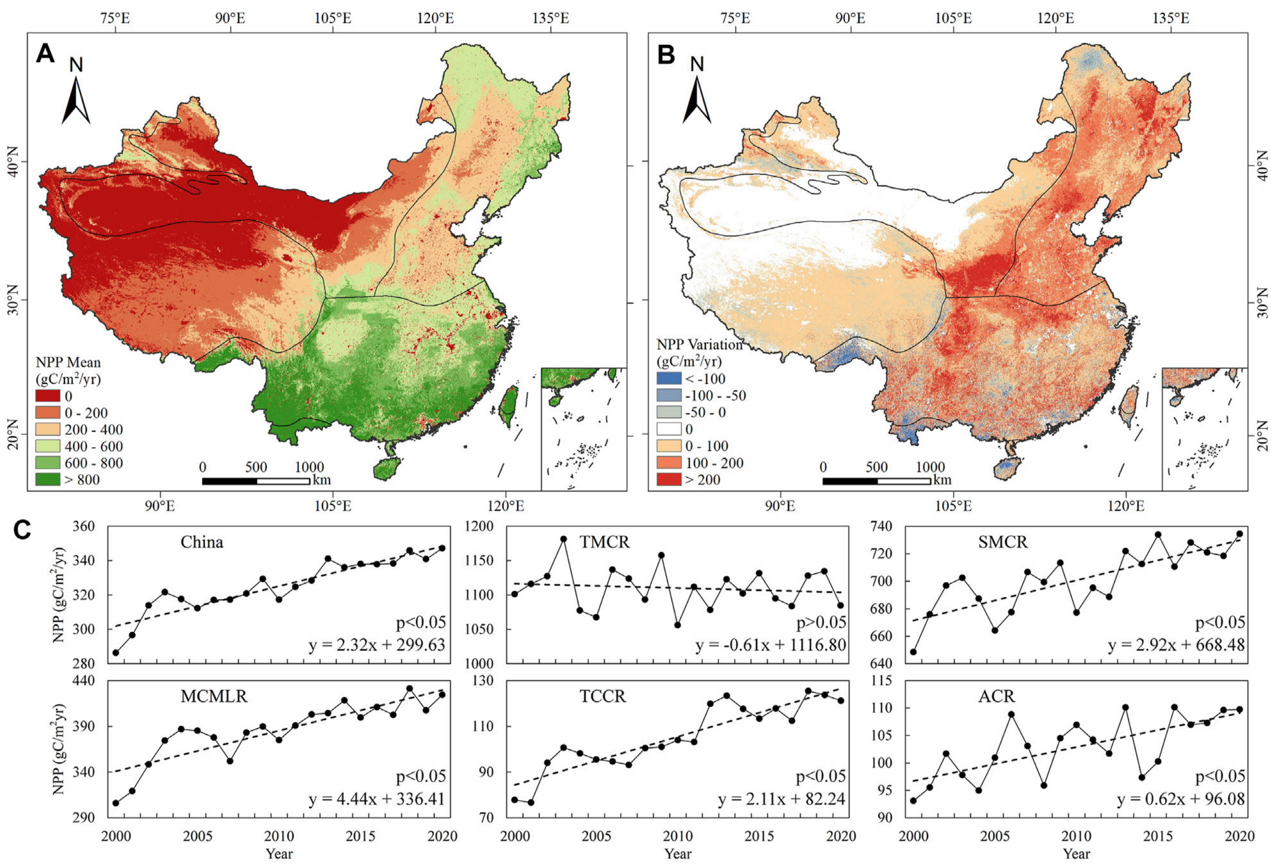

FIGURE 2
Spatial distribution of **(A)** annual average NPP, **(B)** NPP variations, and **(C)** NPP inter-annual variations in China and five sub-regions from 2000 to 2020.

precipitation accounted for 54.06% of China (Figure 4B), mainly including Sichuan Basin, the Loess Plateau, and the Mongolian Plateau, whereas areas with negative contributions of precipitation accounted for 20.41% and were mainly distributed in the Qinghai-Tibetan Plateau, central and southeastern China. Solar radiation made positive contributions in 53.25% of China and negative contributions in 21.24% of China (Figure 4C). Moreover, areas of contributions of solar radiation were similar to that of precipitation. Additionally, positive contributions of human activities were scattered in most areas of China (55.67%) (Figure 4E). However, negative contributions of human activities were mainly distributed in the Qinghai-Tibetan Plateau, the southern Yunnan-Kweichow Plateau, and southeastern China.

3.3 The relative impacts of climate factors and human activities on NPP

Figure 5 shows the spatial distribution of the contribution ratio of climate factors and human activities to NPP change trend from 2000 to 2020. Excluding stable area which accounted for 25.56% of China, areas with the contribution ratio of climate factors greater than 70% were mainly scattered in the Qinghai-Tibetan Plateau, Sichuan Basin, northwestern, and northeastern China, accounted for 24.86% of China (Figure 5A). The area percentage of the contribution ratio of climate factors from 30% to 70% was 21.41%. And the area percentage where the contribution ratio of climate factors less than 30% was 28.17%. Moreover, in 27.57% of China, mainly including central and southeastern China, the contribution ratio of human activities exceeded 70% (Figure 5B). The contribution ratio of human activities of 21.55% of China ranged from 30% to 70%, and 25.32% of China had a contribution ratio less than 30% of human activities.

As shown in Table 2, the contribution ratio of climate factors and human activities to NPP trend was discussed outside of stable area, which was calculated from the average contributions of climate factors and human activities in each sub-region. Overall, climate factors contributed 50.58% to NPP changes. Human activities were the main drivers of NPP changes in TMCR (65.70%) and SMCR (59.21%), while climate factors were the key factors in MCMLR (53.84%), TCCR (50.80%), and ACR (72.28%). In areas with NPP recovery, climate factors dominated in all sub-regions except for SMCR. In areas with NPP degradation, climate factors played a major role in TCCR and ACR, while the contribution ratios of human activities were higher in TMCR, SMCR and MCMLR.

Figure 6 shows the area affected by both climate factors and human activities accounted for 49.84% of China. NPP changes were dominated by climate factors in 13.67% of China, while NPP

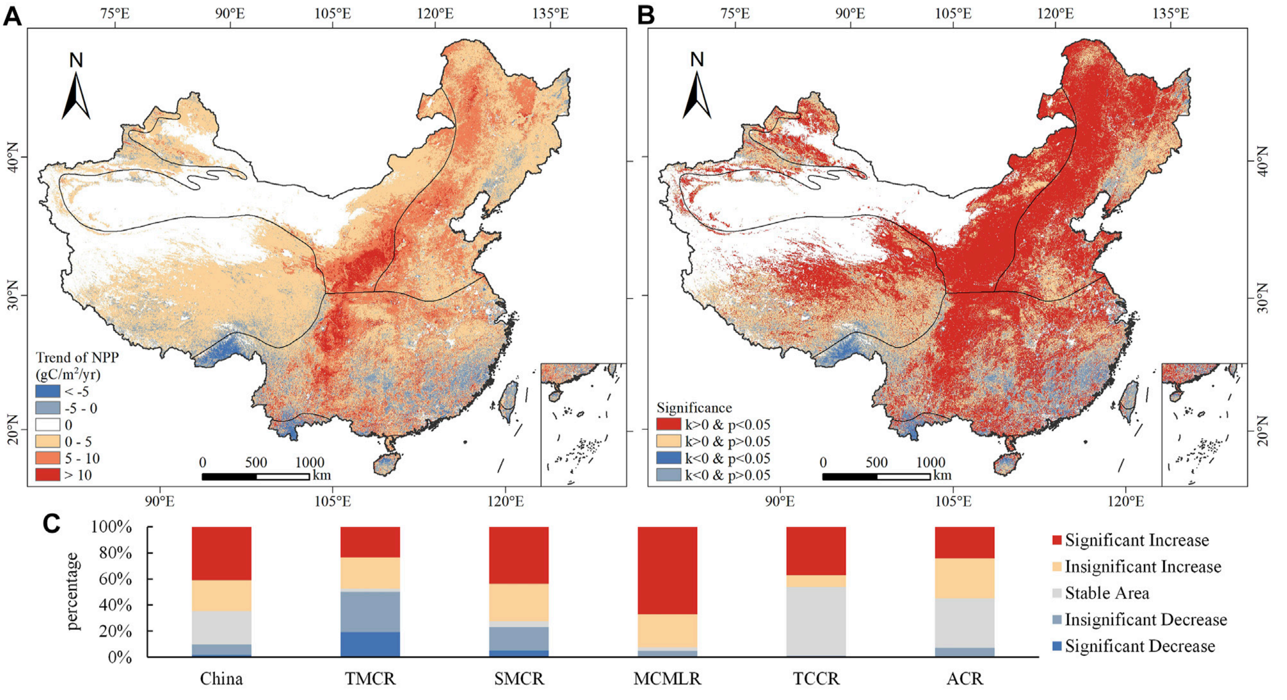

FIGURE 3
(A) Annual change trend of NPP and **(B)** the corresponding significance. **(C)** Statistical results of the percentage changes of NPP for different regions. The legend of **(C)** is the same as that of **(B)**, and stable area means that trend of NPP is 0 or no vegetation.

changes in 10.92% of China were human-dominated. Driving factors of NPP recovery and degradation showed spatial differences in China. On the spatial distribution (Figure 6A), the RC was mainly scattered in the eastern Qinghai-Tibetan Plateau, Sichuan basin, the Mongolian Plateau, and northeastern China. The RH was mainly distributed in central China. And the RB occurred in most areas of China. In contrast, the DC was mainly distributed in the southern flank of the East Himalayas and Taiwan Island. The DH mainly appeared in the southern Yunnan-Kweichow Plateau and southeastern China. And the DB mainly occurred in the southern Qinghai-Tibetan Plateau, the southern Yunnan-Kweichow Plateau, and southeastern China.

Figure 6B shows the area percentage of NPP changes caused by climate factors and human activities. Areas of increases of NPP in which the driving factors were both factors accounted for 45.23%, while areas in which increases of NPP were caused by climate factors and human activities accounted for 11.29% and 8.02%, respectively. However, both factors caused decreases of NPP in 4.61% of China, whereas areas affected by climate factors and human activities in 2.39% and 2.90% of China with such decreases. Both climate factors and human activities were the most important factors for increases of NPP in five sub-regions. The second most important factors for increases of NPP in TMCR, MCMLR, TCCR, and ACR were climate factors, and in SMCR were human activities. In addition, the major driving factors of NPP decreases in TMCR, SMCR, MCMLR, and TCCR were both climate factors and human activities, and in ACR were human activities. The secondary driving factors of NPP decreases in TMCR, SMCR, MCMLR, and TCCR were human activities, and in ACR were both factors.

3.4 Variations of NPP under different types of land cover

We first divided land cover types in China into unchanged and changed land cover types from 2001 to 2020. As shown in Table 3, from 2001 to 2020, the area percentage of unchanged and changed land cover types in China were 92.71% and 7.29%, respectively. The mean NPP of unchanged land cover types increased by 16.48%, while the mean NPP of changed land cover types increased by 24.46%. The statistic total NPP showed that the total NPP percentage of unchanged land cover types in both years was approximately 93% of the overall. In terms of change, the total NPP for the entire China rose by 495.70 Tg C/year, with the increase of total NPP of unchanged land cover types accounting for 90.04% of the overall increase. Therefore, we focused on the analysis of unchanged land cover types due to their contribution to NPP and its growth.

As shown in Figure 7A, forestland (28.08%) and grassland (27.41%) were the most extensive land cover types. Most forestland was located in the southern and northeastern regions of China, and grassland was mainly distributed in the northern and northwestern regions. Farmland was concentrated on the central and northeastern China. Unused land was mainly located in northwestern China. Among the unchanged land cover types, the highest mean NPP was found in forestland, followed by farmland and grassland, and the lowest in water (Figure 7B). The mean NPP

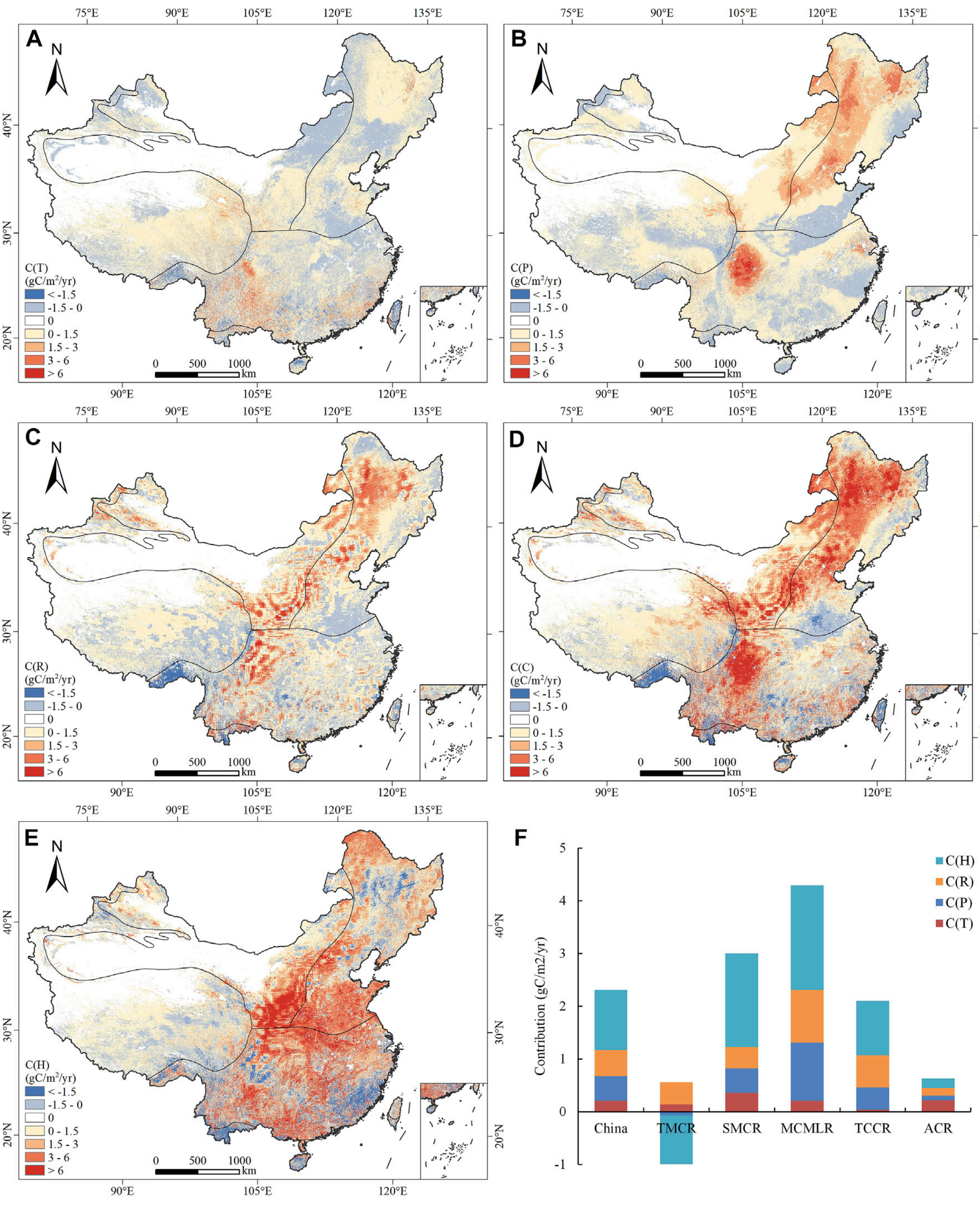

FIGURE 4
The contributions of climate factors [**(A)** temperature, **(B)** precipitation, **(C)** solar radiation, **(D)** climate] and **(E)** human activities to NPP trend from 2000 to 2020. **(F)** The average contributions of climate factors and human activities in China and five sub-regions.

for each of the six land cover types increased from 2001 to 2020. The highest increase in mean NPP was observed in farmland with 110.34 g C/m^2/year, and mean NPP of forestland and grassland increased by 63.46 g C/m^2/year and 55.77 g C/m^2/year, respectively. The total NPP showed a similar trend as the mean NPP. Forestland had the highest total NPP increase with 174.12 Tg C/year, while grassland and farmland were followed with 149.36 Tg C/year and 120.69 Tg C/year of total NPP increase, respectively.

4 Discussion

4.1 Evaluation of the NPP results

In previous studies, Ji et al. (2008) estimated the averaged total NPP of China over 1981-2000 with 2.94 Pg C. During the same period, Peng et al. (2021) determined the NPP by CABLE2.1 and TRENDY ensemble in China varied between 2.7 and 4.0 Pg C. Wang

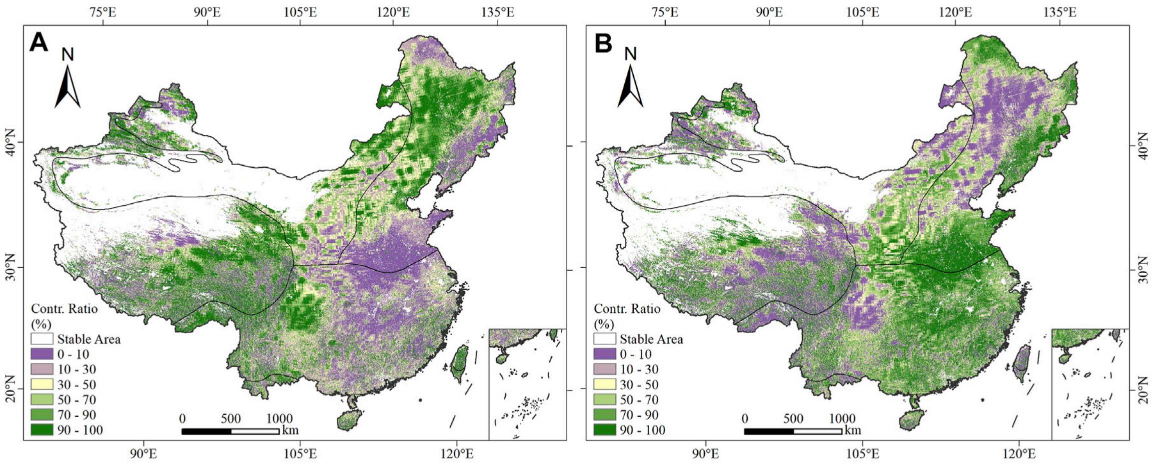

FIGURE 5
Spatial distribution of the contribution ratio of **(A)** climate factors and **(B)** human activities.

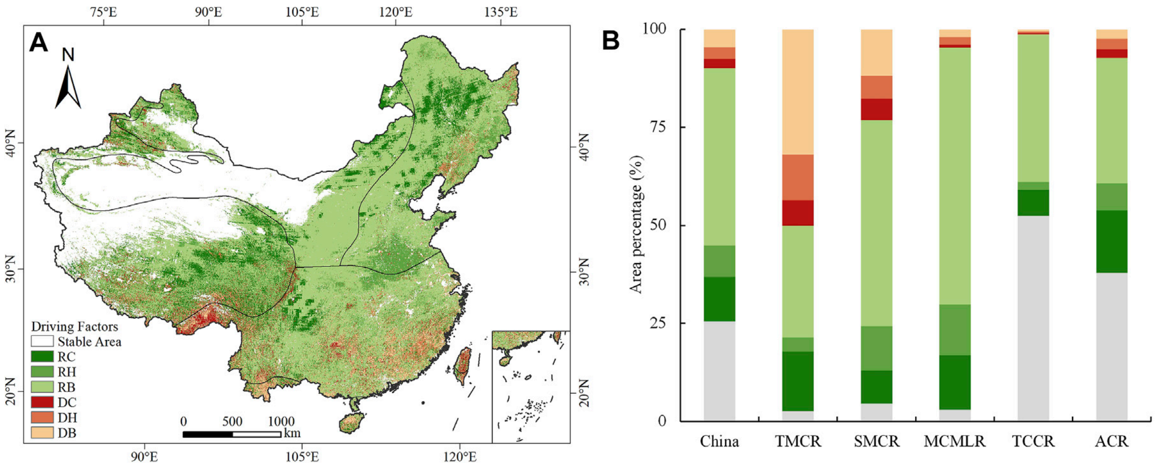

FIGURE 6
(A) Spatial distribution of driving factors to NPP. **(B)** Area percentage of NPP dynamics affected by climate factors and human activities for China and five sub-regions. RC, Recovery for climate factors; RH, Recovery for human activities; RB, Recovery for both factors; DC: Degradation for climate factors; DH, Degradation for human activities; DB, Degradation for both factors. The legend of **(B)** is the same as that of **(A)**.

TABLE 3 Mean and total NPP changes of land cover types from 2001 to 2020.

Land cover type	Area (km^2)	Mean NPP (g C/m^2/year)			Total NPP (Tg C/year)		
		2001	2020	Difference	2001	2020	Difference
Unchanged types	9057669	298.91	348.19	+49.27	2707.45	3153.76	+446.31
Changed types	712195	283.56	352.90	+69.35	201.95	251.34	+49.39
Total area	9769864	297.79	348.53	+50.74	2909.40	3405.10	+495.70

J. et al. (2017) calculated the average total NPP from 37 existing NPP data sets in China from 2000 to 2012 with 2.92 ± 0.12 Pg C. Liu et al. (2022) estimated the annual total NPP of vegetation in China's terrestrial ecosystems varied between 2.72 and 3.29 Pg C from 2000 to 2019, with a multiyear average of 3.09 Pg C. In this study, the total NPP from 2000 to 2020 in China estimated

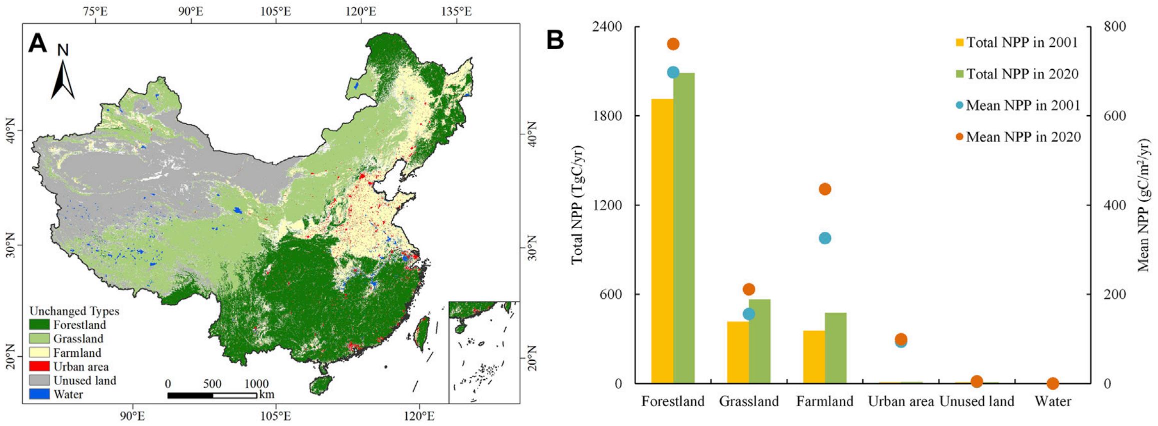

FIGURE 7
(A) Spatial distribution and **(B)** statistics of mean and total NPP variations of the unchanged land cover types from 2001 to 2020.

ranged from 2.81 to 3.41 Pg C, with results consistent with these values. Overall, the trend of total NPP was 0.023 Pg C/year, similar to previous findings (Lai et al., 2018; Liu et al., 2022), who found rates of 0.025 and 0.022 Pg C/year, respectively. For the spatial dimension, pixels with a positive trend in NPP accounted for most of the total pixels, consistent with previous studies (Yang et al., 2017; Ge et al., 2021). The significant decline of NPP mainly occurred in the southern Qinghai-Tibetan Plateau and the southern Yunnan-Kweichow Plateau, which was also found by Luo et al. (2018) and Wang J. et al. (2017), with NPP also showing a decreasing trend in southeastern China (Wen et al., 2019).

4.2 Impacts of climate factors on NPP changes

Climate change was identified as the main drivers affecting NPP distribution and dynamics (Song and Ma, 2011; Liu et al., 2015). Changes in temperature, precipitation and solar radiation affected NPP by altering soil moisture and soil microorganisms, affecting vegetation respiration and photosynthesis (Horion et al., 2013; He et al., 2015). Overall, climate factors contributed positively in 59.45% of China and negatively in 15.05%, which had spatial heterogeneities in the impact of NPP (Figures 4, 8).

For most of the forestland in southern China, due to sufficient precipitation and high temperature in the growing season, vegetation cover represented by NDVI increased, and there was a correlation between NPP and NDVI (Sun et al., 2002), which led to the increase in NPP. Adequate precipitation also enhanced the carbon sequestration capacity of forestland in the Sichuan Basin to increase NPP (Chen et al., 2021a; Wang et al., 2021a). The NPP of forestland in the Greater Khingan Mountains and the Changbai Mountains in northeastern China was positively correlated with temperature and solar radiation, with temperature being the main limiting factor for vegetation growth in the cold temperate region, while increased solar radiation would also enhance vegetation photosynthetic capacity (Yan et al., 2021). The southern Qinghai-Tibetan Plateau showed a decreasing trend of NPP, mainly distributed in subtropical broad-leaved forest with good water and heat conditions. Therefore, the effects of temperature and precipitation on the growth of vegetation in the region was considered to have reached equilibrium or saturation. In the event of significant climate change, the growth of vegetation will be inhibited (Deng et al., 2022). In the southern Yunnan-Kweichow Plateau, precipitation was the most important factor of NPP dynamics in the region’s tropical seasonal rainforests (Linger et al., 2020), and there was a warm-dry trend in climate here that enhanced the effect of drought on NPP decline (Zhou et al., 2022). The increase in vapor pressure deficit and temperature greatly increased the demand for atmospheric evaporation, further causing vegetation stomata to close, resulting in lower leaf intercellular CO_2 concentrations and limiting photosynthesis (Li et al., 2010).

Temperature and solar radiation were the dominant climatic factors affecting grassland growth in the Qinghai-Tibetan Plateau (Xu et al., 2016). In the central and eastern Qinghai-Tibetan Plateau, warmer temperature contributed positively to the increase of NPP of alpine grassland because of a lengthened growing season and a more rapid rate of photosynthesis (Gu et al., 2017), and there was also a significant positive correlation between solar radiation and NPP of grassland, where plant chlorophyll content was increased and photosynthesis was enhanced (Meng et al., 2020). Conversely, temperature and solar radiation were negatively correlated with NPP at higher elevations in the western Qinghai-Tibetan Plateau, possibly because increases in temperature led to melting of snow and permafrost, which disrupted the structure of vegetative root systems and hindered grassland growth (Xiong et al., 2016). In addition, excessive solar radiation increased evaporation of surface soil and limited water availability, which may prevent the growth of herbaceous plants with shallow root systems (Yang et al., 2017). Precipitation had a suppressive effect on grassland growth in southeastern plateau (Gao et al., 2013; Xiong et al., 2021), and its increase may reduce solar radiation, which inhibits photosynthesis (Yang et al., 2015). Alternatively, precipitation could contribute to soil erosion, which decreased soil organic matter content, and reduced alpine grassland NPP (Xu et al., 2016). In arid and semi-arid areas, e.g., the Mongolian Plateau and the Loess Plateau,

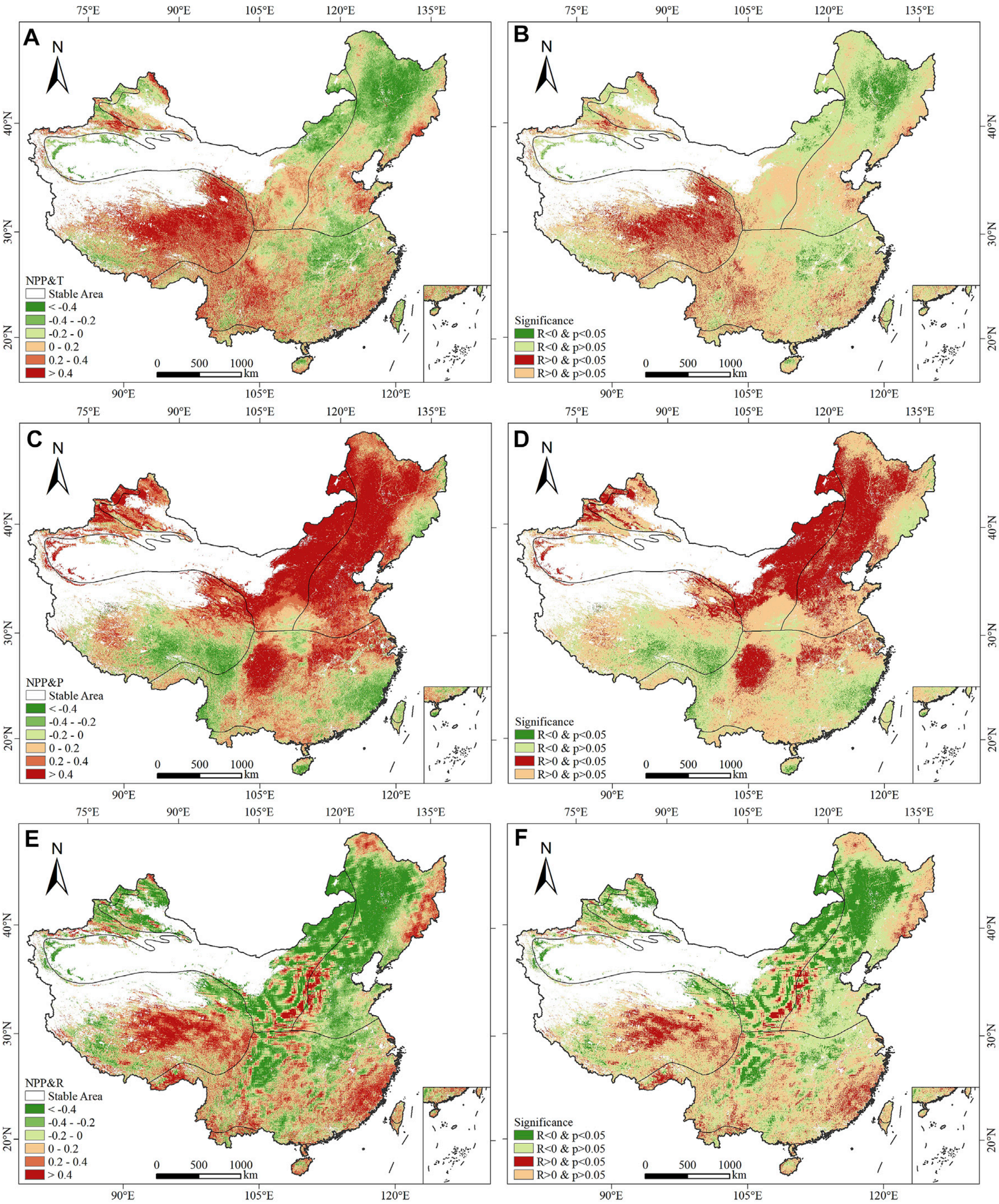

FIGURE 8
Spatial distribution of the correlation coefficients between NPP and **(A)** temperature, **(C)** precipitation, **(E)** solar radiation and **(B,D,F)** their corresponding significance.

precipitation was an important controlling driver of grassland growth which was confirmed in the previous studies (Zhao et al., 2019; Jiang H. et al., 2020; Wu N. et al., 2021). NPP was negatively correlated with temperature in the arid land of the Mongolian Plateau, mainly due to the fact that warming exacerbated the negative effects of drought on grassland growth (Zeng and Yang, 2008).

In the northeast agricultural region of China, the average temperature of growing season met the requirements of the first few stages of crop growth, but at maturity, it exceeded the optimum temperature for crop growth, while the average precipitation of growing season did not exceed the optimum humidity (Piao et al., 2010). Therefore, NPP showed a positive correlation with precipitation and a negative correlation with temperature. In addition, in central China, due to excessive warmth and decrease in precipitation, the photosynthesis of plants was weakened, resulting in a negative contribution to farmland NPP (Chen et al., 2021b).

In addition, droughts are a comprehensive and frequently occurred natural disaster affected by multiple climate factors, and will greatly influence vegetation growth and reduce the net primary production (Zhao and Running, 2010; van der Molen et al., 2011). During drought, soil water content decreased and vegetation stomata closed, thus limiting plant growth (van der Molen et al., 2011; Chen et al., 2013; Su et al., 2018). Drought also indirectly affected ecosystem productivity by increasing pest and disease infestation and causing forest fires (Xiao and Zhuang, 2007; Anderegg et al., 2013). Previous studies have shown that five typical drought events occurred in China from 1982 to 2015, resulting in a decline in NPP in more than 23% of the area (Lai et al., 2018), and the effects of drought on NPP were mainly located in farming-pastoral ecotones of arid and semi-arid ecosystems (Li et al., 2020). Although with strong carbon sequestration capacity, vegetation growth in southwestern China was highly vulnerable to drought suppression, and the effects of drought on ecosystem water-use efficiency were seasonal, which affected ecosystem productivity (Wang et al., 2021b). In this area, in a region with complicated and fragmentized topography, drought may not evidently decrease the NPP, but may enormously impact NPP in a region with overall flat topography (Guan et al., 2018).

For some regional studies in neighboring China, in the Western Himalaya, the land cover type in India was mainly forestland, while in China it was dominated by unused land and grassland. Due to the difference in vegetation types as well as hydrothermal conditions between the two regions, NPP variation in the Indian Western Himalayan region was negatively correlated with temperature (Kumar et al., 2019), while it was positively in the Chinese Western Himalayan region (Figure 8). However, precipitation and solar radiation exhibited a consistent trend with NPP change in both regions (Sharma et al., 2022). Central Asia and northwest China were both arid and semi-arid zones with temperate continental climate, and precipitation was the main climatic driver controlling the NPP variations in most areas of both regions (Jiang et al., 2017; Chen T. et al., 2019). The Lancang-Mekong River was known as the Lancang River in China and the Mekong River in Southeast Asia. In the Lancang River basin, where hydrothermal conditions were poor, the correlation between NPP and temperature was positive. In contrast, NPP was negatively correlated with temperature in the Mekong River Basin where good hydrothermal conditions existed, and the correlation between NPP and precipitation in space was not obvious (Li W. et al., 2018).

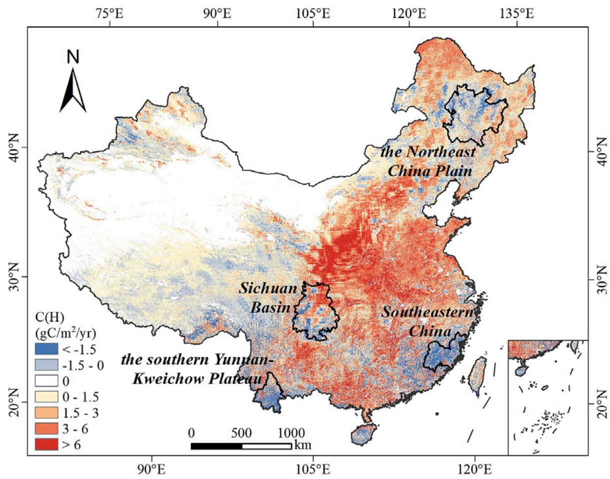

FIGURE 9
The contribution map of human activities to NPP trend from 2000 to 2020 and four typical regions with high negative contributions in Sichuan Basin, the southern Yunnan-Kweichow Plateau, southeastern China, and the Northeast China Plain.

4.3 Impacts of human activities on NPP changes

Human activities were also significant factors affecting the recovery or degradation of vegetation (Cai et al., 2015; Naeem et al., 2020). In arid and semi-arid regions of northwestern China, human activities were the dominant driving factors in desertification development (Zhang et al., 2011; Zhou et al., 2015). Human activities including overgrazing, overuse of water resources and deforestation have caused damage to natural vegetation, leading to desertification expansion (Li et al., 2016; Li C. et al., 2021). Grazing affected biomass through feeding, affected the physical structure of the soil through trampling, making bare topsoil vulnerable to erosion by strong wind (Jiang H. et al., 2020). In recent decades, with the implementation of a series of ecological restoration projects like the Grain to Green Program (GTGP) and Grazing Withdrawal Program (GWP), the vegetation in the northwestern China has been well protected and restored (Liu et al., 2019a). The GTGP was launched in 1999 to replace cropland and grazing land with grassland and woodland in fragile regions (Mu et al., 2013) and the GWP was initiated in 2003 to reduce the grazing pressure on natural grassland by forbidding grazing and employing cultivated pastures (Xu et al., 2016), which contributed positively to the Qinghai-Tibet Plateau, the Loess Plateau, the Mongolian Plateau, and Xinjiang Uygur Autonomous Region on vegetation restoration (Yang et al., 2014; Cai et al., 2015; Gang et al., 2018; Shi et al., 2022).

In the North China Plain and the Middle and Lower Yangtze River Plain, human cultivation activities contributed to NPP increases (Ge et al., 2021), and were mainly manifested in the improvement of agricultural machinery level, technology and investment, which improved the efficiency and mechanization of farm irrigation and promoted the development of cultivated land quality. The Natural Forest Protection Program aimed to prohibit logging in the southwest China and significantly reduce deforestation in the northeast China and other natural forest areas (Xu et al., 2006), which has reduced soil erosion and improved vegetation conditions in the Hengduan Mountain and the Greater Khingan Mountains (Yin et al., 2020).

With socio-economic development, land cover and use have changed dramatically at the same time, which will affect the ecological environment (Yang et al., 2021). We selected four typical regions with high negative contribution of human

TABLE 4 Land cover changes in four typical regions from 2001 to 2020 (unit: km^2).

Area	Land cover	Translates to						
		Forestland	Grassland	Farmland	Urban area	Unused land	Water	Total
Sichuan Basin	Forestland	20276	1,230	21	11	0	0	21538
	Grassland	8852	58650	19592	782	16	284	88176
	Farmland	15	8373	47275	1,590	1	2	57256
	Urban area	0	0	0	2869	0	0	2869
	Unused land	0	49	0	8	74	17	148
	Water	5	169	18	19	4	177	392
	Total	29148	68471	66906	5279	95	480	170379
Southern Yunnan-Kweichow Plateau	Forestland	60337	169	195	7	1	3	60712
	Grassland	420	62	53	0	0	9	544
	Farmland	578	58	703	1	0	6	1,346
	Urban area	0	0	0	140	0	0	140
	Unused land	0	0	0	0	0	0	0
	Water	0	0	0	0	0	0	0
	Total	61335	289	951	148	1	18	62742
South-eastern China	Forestland	76294	619	115	503	0	4	77535
	Grassland	333	381	13	48	9	0	784
	Farmland	321	89	555	208	0	0	1,173
	Urban area	0	0	0	3307	0	0	3307
	Unused land	0	3	0	2	17	0	22
	Water	0	1	0	0	0	276	277
	Total	76948	1,093	683	4068	26	280	83098
Northeast China Plain	Forestland	31077	369	475	2	0	2	31925
	Grassland	532	39179	19427	79	168	377	59762
	Farmland	1856	2736	130690	409	10	236	135937

(Continued on following page)

TABLE 4 (*Continued*) Land cover changes in four typical regions from 2001 to 2020 (unit: km²).

Area	Land cover	Translates to						
		Forestland	Grassland	Farmland	Urban area	Unused land	Water	Total
	Urban area	0	0	0	3183	0	0	3183
	Unused land	0	302	2	1	177	156	638
	Water	0	57	3	0	13	1,286	1,359
	Total	33465	42643	150597	3674	368	2057	232804

activities for analysis, including Sichuan Basin, the southern Yunnan-Kweichow Plateau, southeastern China, and the Northeast China Plain (Figure 9). During the study period, land cover changed significantly in these regions (Table 4). In Sichuan Basin, 22.22% of grassland and 5.71% of forestland translated to farmland, and urban area increased by 84.00%. Similarly, urban area in the Northeast China Plain increased by 15.43%, and 32.51% of grassland translated to farmland, which meant human agricultural activities with the conversion of large amounts of grassland to farmland may lead to a decrease in NPP (Tian et al., 2020; Li H. et al., 2021). In southeastern China, which was one of the more economically developed regions in China, urban area increased by 23.01%, and 17.73% of farmland translated to urban area. Several studies have shown that the process of urbanization has caused a certain degree of damage to the ecological environment (Wu et al., 2014; Liu X. et al., 2019).

Moreover, continuous urban expansion, rapid economic development, and sustained population growth were also considered to be factors affecting NPP (Ma et al., 2012; Li et al., 2022). Generally, these four typical regions experienced rapid economic development from 2000 to 2020, and the average annual rates of GDP growth in Sichuan Basin, the southern Yunnan-Kweichow Plateau, southeastern China, and the Northeast China Plain were 13.95%, 14.81%, 13.12%, and 8.67%, respectively. Regional population size was often cited as the main reason for the decline in ecosystem services, and GDP density growth inevitably limits NPP increase (Cincotta et al., 2000; Qiu et al., 2018). In addition, ecological damage in the southern Yunnan-Kweichow Plateau was mainly caused by high-intensity development activities such as tourism (Tang et al., 2015).

4.4 Limitations of this study

It should be noted that some uncertainties existed in this study. First, MODIS NPP data may contain some uncertainties owing to the lack of site-level measured data, which had some impacts on the results of study. Nevertheless, the dataset has been proven to be reliable in previous studies (Peng et al., 2016; Liu et al., 2019b), and has been widely used in research on global and regional NPP (Zhao et al., 2005; Zhang et al., 2014; Sha et al., 2020). Second, MODIS NPP data and land cover data were both resampled to 1,000 m, which sacrifices accuracy to some extent, resulting in each pixel potentially not reflecting the actual land cover types (Shen et al., 2020; Shen et al., 2022). Third, in MODIS NPP data, the NPP value of water, barren land, urban/built-up was 0. However, the classification of the land cover data used in this study may not correspond exactly to the classification used in the MODIS NPP data, resulting in non-zero values of mean NPP for water, unused land, and urban area counted in this study. Fourth, in this study, only three climate factors, temperature, precipitation, and solar radiation, were considered, while other factors such as CO_2 concentration, Nitrogen deposition, and soil moisture were ignored, which also affected vegetation NPP dynamics (Mu et al., 2008; Du et al., 2014; He et al., 2017). Finally, the method (RESTREND) used in this study ignores the complex interactions between climate change and human activities, and only considers the linear relationship between NPP and impact factors. Although the method has some shortcomings, its ability to quantify the relative contributions of vegetation dynamics drivers is significant for understanding the driving mechanisms.

5 Conclusion

In this study, we investigated spatiotemporal characteristics of NPP in China from 2000 to 2020. The influences of climate factors and human activities on NPP were also analyzed quantitatively. The main conclusions are summarized as follows:

(1) The annual average NPP of the entire China increased from 2000 (286.31 g C/m^2/year) to 2020 (348.53 g C/m^2/year) at a rate of 2.32 g C/m^2/year, and a total NPP increase of 596.73 Tg C/year was found. Areas of significant increase in NPP accounted for 40.90% of China, with only 1.79% showing a significant declining trend.
(2) Climate factors contributed more to NPP variations in China from 2000 to 2020 than human activities, and the contributions of climate factors and human activities were 1.169 g C/m^2/year and 1.142 g C/m^2/year. In terms of NPP recovery, NPP was dominated by both climate factors and human activities in 45.23% of China. Regarding NPP degradation, areas dominated by both factors, climate factors, and human activities accounted for 4.61%, 2.39%, and 2.90%, respectively.
(3) The proportion of area with unchanged land cover types was 92.71% of the entire China. The total NPP increase of unchanged land cover types accounted for 90.04% of the total increase, and was mainly contributed by forestland, grassland and farmland.

Overall, both climate factors and human activities have contributed to NPP variation in China. The results improve the understanding of how ecosystems in China have been affected by climate factors and human activities in the last two decades, and also provide guidance for formulating ecosystem management and governance strategies to protect the environment and achieve sustainable development.

Data availability statement

The original contributions presented in the study are included in the article/supplementary material, further inquiries can be directed to the corresponding authors.

Author contributions

Conceptualization, JC and ZPC; Methodology, JC and ZS; Software, JY and ZTC; data collection, ZL and ZTC; Funding acquisition, ZPC and ZS; Supervision, JC and ZPC; Writing—original draft preparation, ZL; Writing—review and editing, ZL, JC, and JY. All authors read and approved the submitted version.

Funding

This work was supported by the Key Laboratory of Natural Resources Monitoring in Tropical and Subtropical Area of South China, Ministry of Natural Resources (No. 2022NRM006) and the Open Fund of Key Laboratory of National Geographical Census and Monitoring, Ministry of Natural Resources (No. 2022NGCM02).

Conflict of interest

The authors declare that the research was conducted in the absence of any commercial or financial relationships that could be construed as a potential conflict of interest.

Publisher's note

References

Anderegg, W. R. L., Kane, J. M., and Anderegg, L. D. L. (2013). Consequences of widespread tree Mortality triggered by drought and temperature stress. *Nat. Clim. Change* 3 (1), 30–36. doi:10.1038/nclimate1635

Cai, H., Yang, X., and Xu, X. (2015). Human-induced grassland degradation/restoration in the central Tibetan Plateau: The effects of ecological protection and restoration projects. *Ecol. Eng.* 83, 112–119. doi:10.1016/j.ecoleng.2015.06.031

Chen, B., Zhang, X., Tao, J., Wu, J., Wang, J., Shi, P., et al. (2014). The impact of climate change and anthropogenic activities on alpine grassland over the Qinghai-Tibet Plateau. *Agric. For. Meteorol.* 189, 11–18. doi:10.1016/j.agrformet.2014.01.002

Chen, S., Wen, Z., Ma, M., and Wu, S. (2021a). Disentangling climatic factors and human activities in governing the old and new forest productivity. *Remote Sens.* 13 (18), 3746. doi:10.3390/rs13183746

Chen, S., Zhang, Y., Wu, Q., Liu, S., Song, C., Xiao, J., et al. (2021b). Vegetation structural change and CO2 fertilization more than offset gross primary production decline caused by reduced solar radiation in China. *Agric. For. Meteorol.* 296, 108207. doi:10.1016/j.agrformet.2020.108207

Chen, T., Bao, A., Jiapaer, G., Guo, H., Zheng, G., Jiang, L., et al. (2019). Disentangling the relative impacts of climate change and human activities on arid and semiarid grasslands in Central Asia during 1982-2015. *Sci. Total Environ.* 653, 1311–1325. doi:10.1016/j.scitotenv.2018.11.058

Chen, T., Werf, G. R. V. D., Jeu, R. A. M. D., Wang, G., and Dolman, A. J. (2013). A global analysis of the impact of drought on net primary productivity. *Hydrol. Earth Syst. Sci.* 17 (10), 3885–3894. doi:10.5194/hess-17-3885-2013

Chen, Y., Gu, H., Wang, M., Gu, Q., Ding, Z., Ma, M., et al. (2019). Contrasting performance of the remotely-derived GPP products over different climate zones across China. *Remote Sens.* 11 (16), 1855. doi:10.3390/rs11161855

Chi, D., Wang, H., Li, X., Liu, H., and Li, X. (2018). Assessing the effects of grazing on variations of vegetation NPP in the Xilingol Grassland, China, using a grazing pressure index. *Ecol. Indic.* 88, 372–383. doi:10.1016/j.ecolind.2018.01.051

Churkina, G., and Running, S. W. (1998). Contrasting climatic controls on the estimated productivity of global terrestrial biomes. *Ecosystems* 1 (2), 206–215. doi:10.1007/s100219900016

Cincotta, R. P., Wisnewski, J., and Engelman, R. (2000). Human population in the biodiversity hotspots. *Nature* 404 (6781), 990–992. doi:10.1038/35010105

Crabtree, R., Potter, C., Mullen, R., Sheldon, J., Huang, S. L., Harmsen, J., et al. (2009). A modeling and spatio-temporal analysis framework for monitoring environmental change using NPP as an ecosystem indicator. *Remote Sens. Environ.* 113 (7), 1486–1496. doi:10.1016/j.rse.2008.12.014

Cramer, W., Kicklighter, D. W., Bondeau, A., Moore, B., Churkina, G., Nemry, B., et al. (1999). Comparing global models of terrestrial net primary productivity (NPP): Overview and key results. *Glob. Change Biol.* 5, 1–15. doi:10.1046/j.1365-2486.1999.00009.x

Dameneh, H. E., Gholami, H., Telfer, M. W., Comino, J. R., Collins, A. L., and Jansen, J. D. (2021). Desertification of Iran in the early twenty-first century: Assessment using climate and vegetation indices. *Sci. Rep.* 11 (1), 20548. doi:10.1038/s41598-021-99636-8

Deng, X., Wu, L., He, C., and Shao, H. (2022). Study on spatiotemporal variation pattern of vegetation coverage on Qinghai-Tibet Plateau and the analysis of its climate driving factors. *Int. J. Environ. Res. Public Health* 19 (14), 8836. doi:10.3390/ijerph19148836

Du, Z., Wang, W., Zeng, W., and Zeng, H. (2014). Nitrogen deposition enhances carbon sequestration by plantations in northern China. *PLoS One* 9 (2), e87975. doi:10.1371/journal.pone.0087975

Dusenge, M. E., Duarte, A. G., and Way, D. A. (2019). Plant carbon metabolism and climate change: Elevated CO2 and temperature impacts on photosynthesis, photorespiration and respiration. *New Phytol.* 221 (1), 32–49. doi:10.1111/nph.15283

Evans, J., and Geerken, R. (2004). Discrimination between climate and human-induced dryland degradation. *J. Arid. Environ.* 57 (4), 535–554. doi:10.1016/S0140-1963(03)00121-6

Feng, X., Fu, B., Lu, N., Zeng, Y., and Wu, B. (2013). How ecological restoration alters ecosystem services: An analysis of carbon sequestration in China's Loess Plateau. *Sci. Rep.* 3, 2846. doi:10.1038/srep02846

Gang, C., Gao, X., Peng, S., Chen, M., Guo, L., and Jin, J. (2019). Satellite observations of the recovery of forests and grasslands in western China. *J. Geophys. Res. Biogeo.* 124 (7), 1905–1922. doi:10.1029/2019JG005198

Gang, C., Zhao, W., Zhao, T., Zhang, Y., Gao, X., and Wen, Z. (2018). The impacts of land conversion and management measures on the grassland net primary productivity over the Loess Plateau, Northern China. *Sci. Total Environ.* 645, 827–836. doi:10.1016/j.scitotenv.2018.07.161

Gao, Y., Zhou, X., Wang, Q., Wang, C., Zhan, Z., Chen, L., et al. (2013). Vegetation net primary productivity and its response to climate change during 2001-2008 in the Tibetan Plateau. *Sci. Total Environ.* 444, 356–362. doi:10.1016/j.scitotenv.2012.12.014

Ge, W., Deng, L., Wang, F., and Han, J. (2021). Quantifying the contributions of human activities and climate change to vegetation net primary productivity dynamics in China from 2001 to 2016. *Sci. Total Environ.* 773, 145648. doi:10.1016/j.scitotenv.2021.145648

Gower, S. T., Kucharik, C. J., and Norman, J. M. (1999). Direct and indirect estimation of leaf area index, f(APAR), and net primary production of terrestrial ecosystems. *Remote Sens. Environ.* 70 (1), 29–51. doi:10.1016/S0034-4257(99)00056-5

Gu, F., Zhang, Y., Huang, M., Tao, B., Guo, R., and Yan, C. (2017). Effects of climate warming on net primary productivity in China during 1961-2010. *Ecol. Evol.* 7 (17), 6736–6746. doi:10.1002/ece3.3029

Guan, X., Shen, H., Li, X., Gan, W., and Zhang, L. (2018). Climate control on net primary productivity in the complicated mountainous area: A case study of yunnan, China. *IEEE J. Sel. Top. Appl. Earth Obs. Remote Sens.* 11 (12), 4637–4648. doi:10.1109/JSTARS.2018.2863957

He, C., Tian, J., Gao, B., and Zhao, Y. (2015). Differentiating climate- and human-induced drivers of grassland degradation in the Liao River Basin, China. *Environ. Monit. Assess.* 187 (1), 4199. doi:10.1007/s10661-014-4199-2

He, L., Chen, J., Liu, J., Belair, S., and Luo, X. (2017). Assessment of SMAP soil moisture for global simulation of gross primary production. *J. Geophys. Res. Biogeo.* 122 (7), 1549–1563. doi:10.1002/2016JG003603

Horion, S., Cornet, Y., Erpicum, M., and Tychon, B. (2013). Studying interactions between climate variability and vegetation dynamic using a phenology based approach. *Int. J. Appl. Earth Obs. Geoinf.* 20, 20–32. doi:10.1016/j.jag.2011.12.010

Ji, J., Huang, M., and Li, K. (2008). Prediction of carbon exchanges between China terrestrial ecosystem and atmosphere in 21st century. *Sci. China Ser. D-Earth. Sci.* 51 (6), 885–898. doi:10.1007/s11430-008-0039-y

Jiang, H., Xu, X., Guan, M., Wang, L., Huang, Y., and Jiang, Y. (2020). Determining the contributions of climate change and human activities to vegetation dynamics in agro-pastural transitional zone of northern China from 2000 to 2015. *Sci. Total Environ.* 718, 134871. doi:10.1016/j.scitotenv.2019.134871

Jiang, L., Jiapaer, G., Bao, A., Guo, H., and Ndayisaba, F. (2017). Vegetation dynamics and responses to climate change and human activities in Central Asia. *Sci. Total Environ.* 599, 967–980. doi:10.1016/j.scitotenv.2017.05.012

Jiang, Y., Guo, J., Peng, Q., Guan, Y., Zhang, Y., and Zhang, R. (2020). The effects of climate factors and human activities on net primary productivity in Xinjiang. *Int. J. Biometeorol.* 64 (5), 765–777. doi:10.1007/s00484-020-01866-4

Kumar, M., SavitaSingh, H., Pandey, R., Singh, M. P., Ravindranath, N. H., Kalra, N., et al. (2019). Assessing vulnerability of forest ecosystem in the Indian Western Himalayan region using trends of net primary productivity. *Biodivers. Conserv.* 28 (8-9), 2163–2182. doi:10.1007/s10531-018-1663-2

Lai, C., Li, J., Wang, Z., Wu, X., Zeng, Z., Chen, X., et al. (2018). Drought-Induced reduction in net primary productivity across mainland China from 1982 to 2015. *Remote Sens.* 10 (9), 1433. doi:10.3390/rs10091433

Li, C., Wang, Y., Wu, X., Cao, H., Li, W., and Wu, T. (2021). Reducing human activity promotes environmental restoration in arid and semi-arid regions: A case study in northwest China. *Sci. Total Environ.* 768, 144525. doi:10.1016/j.scitotenv.2020.144525

Li, D., Xu, D., Wang, Z., You, X., Zhang, X., and Song, A. (2018). The dynamics of sand-Stabilization services in Inner Mongolia, China from 1981 to 2010 and its relationship with climate change and human activities. *Ecol. Indic.* 88, 351–360. doi:10.1016/j.ecolind.2018.01.018

Li, H., Zhang, H., Li, Q., Zhao, J., Guo, X., Ying, H., et al. (2021). Vegetation productivity dynamics in response to climate change and human activities under different topography and land cover in northeast China. *Remote Sens.* 13 (5), 975. doi:10.3390/rs13050975

Li, J., Wang, Y., and Liu, L. (2020). Responses of the terrestrial ecosystem productivity to droughts in China. *Front. Earth Sci.* 8. doi:10.3389/feart.2020.00059

Li, M., Yu, H., Meng, B., Sun, Y., Zhang, J., Zhang, H., et al. (2021a). Drought reduces the effectiveness of ecological projects: Perspectives from the inter-annual variability of vegetation index. *Ecol. Indic.* 130, 108158. doi:10.1016/j.ecolind.2021.108158

Li, M., Zhang, X., Wu, J., Ding, Q., Niu, B., and He, Y. (2021b). Declining human activity intensity on alpine grasslands of the Tibetan Plateau. *J. Environ. Manage.* 296, 113198. doi:10.1016/j.jenvman.2021.113198

Li, Q., Zhang, C., Shen, Y., Jia, W., and Li, J. (2016). Quantitative assessment of the relative roles of climate change and human activities in desertification processes on the Qinghai-Tibet Plateau based on net primary productivity. *Catena* 147, 789–796. doi:10.1016/j.catena.2016.09.005

Li, W., Li, C., Liu, X., He, D., Bao, A., Yi, Q., et al. (2018). Analysis of spatial-temporal variation in NPP based on hydrothermal conditions in the Lancang-Mekong River Basin from 2000 to 2014. *Environ. Monit. Assess.* 190 (6), 321. doi:10.1007/s10661-018-6690-7

Li, X., Luo, Y., and Wu, J. (2022). Decoupling relationship between urbanization and carbon sequestration in the Pearl River Delta from 2000 to 2020. *Remote Sens.* 14 (3), 526. doi:10.3390/rs14030526

Li, Z., Zhang, Y., Wang, S., Yuan, G., Yang, Y., and Cao, M. (2010). Evapotranspiration of a tropical rain forest in Xishuangbanna, southwest China. *Hydrol. Process.* 24 (17), 2405–2416. doi:10.1002/hyp.7643

Linger, E., Hogan, J. A., Cao, M., Zhang, W., Yang, X., and Hu, Y. (2020). Precipitation influences on the net primary productivity of a tropical seasonal rainforest in southwest China: A 9-year case study. *For. Ecol. Manage.* 467, 118153. doi:10.1016/j.foreco.2020.118153

Liu, C., Dong, X., and Liu, Y. (2015). Changes of NPP and their relationship to climate factors based on the transformation of different scales in Gansu, China. *Catena* 125, 190–199. doi:10.1016/j.catena.2014.10.027

Liu, G., Shao, Q., Fan, J., Ning, J., Rong, K., Huang, H., et al. (2022). Change trend and restoration potential of vegetation net primary productivity in China over the past 20 years. *Remote Sens.* 14 (7), 1634. doi:10.3390/rs14071634

Liu, H., Jiao, F., Yin, J., Li, T., Gong, H., Wang, Z., et al. (2020). Nonlinear relationship of vegetation greening with nature and human factors and its forecast - a case study of Southwest China. *Ecol. Indic.* 111, 106009. doi:10.1016/j.ecolind.2019.106009

Liu, Q., Fu, Y., Zhu, Z., Liu, Y., Liu, Z., Huang, M., et al. (2016). Delayed autumn phenology in the Northern Hemisphere is related to change in both climate and spring phenology. *Glob. Change Biol.* 22 (11), 3702–3711. doi:10.1111/gcb.13311

Liu, X., Pei, F., Wen, Y., Li, X., Wang, S., Wu, C., et al. (2019). Global urban expansion offsets climate-driven increases in terrestrial net primary productivity. *Nat. Commun.* 10 (1), 5558. doi:10.1038/s41467-019-13462-1

Liu, Y., Wang, Q., Zhang, Z., Tong, L., Wang, Z., and Li, J. (2019a). Grassland dynamics in responses to climate variation and human activities in China from 2000 to 2013. *Sci. Total Environ.* 690, 27–39. doi:10.1016/j.scitotenv.2019.06.503

Liu, Y., Zhang, Z., Tong, L., Khalifa, M., Wang, Q., Gang, C., et al. (2019b). Assessing the effects of climate variation and human activities on grassland degradation and restoration across the globe. *Ecol. Indic.* 106, 105504. doi:10.1016/j.ecolind.2019.105504

Luo, Z., Wu, W., Yu, X., Song, Q., Yang, J., Wu, J., et al. (2018). Variation of net primary production and its correlation with climate change and anthropogenic activities over the Tibetan plateau. *Remote Sens.* 10 (9), 1352. doi:10.3390/rs10091352

Ma, T., Zhou, C., and Pei, T. (2012). Simulating and estimating tempo-spatial patterns in global human appropriation of net primary production (hanpp): A consumption-based approach. *Ecol. Indic.* 23, 660–667. doi:10.1016/j.ecolind.2012.05.026

Melillo, J. M., Mcguire, A. D., Kicklighter, D. W., Moore, B., Vorosmarty, C. J., and Schloss, A. L. (1993). Global climate-change and terrestrial net primary production. *Nature* 363 (6426), 234–240. doi:10.1038/363234a0

Meng, Z., Liu, M., Gao, C., Zhang, Y., She, Q., Long, L., et al. (2020). Greening and browning of the coastal areas in mainland China: Spatial heterogeneity, seasonal variation and its influential factors. *Ecol. Indic.* 110, 105888. doi:10.1016/j.ecolind.2019.105888

Mu, Q., Zhao, M., Running, S. W., Liu, M., and Tian, H. (2008). Contribution of increasing CO2 and climate change to the carbon cycle in China's ecosystems. *J. Geophys. Res. Biogeo.* 113 (G1). doi:10.1029/2006JG000316

Mu, S., Zhou, S., Chen, Y., Li, J., Ju, W., and Odeh, I. O. A. (2013). Assessing the impact of restoration-induced land conversion and management alternatives on net primary productivity in Inner Mongolian grassland, China. *Glob. Planet. Change* 108, 29–41. doi:10.1016/j.gloplacha.2013.06.007

Naeem, S., Zhang, Y., Tian, J., Qamer, F. M., Latif, A., and Paul, P. K. (2020). Quantifying the impacts of anthropogenic activities and climate variations on vegetation productivity changes in China from 1985 to 2015. *Remote Sens.* 12 (7), 1113. doi:10.3390/rs12071113

Nemani, R. R., Keeling, C. D., Hashimoto, H., Jolly, W. M., Piper, S. C., Tucker, C. J., et al. (2003). Climate-driven increases in global terrestrial net primary production from 1982 to 1999. *Science* 300 (5625), 1560–1563. doi:10.1126/science.1082750

Peng, D., Wu, C., Zhang, B., Huete, A., Zhang, X., Sun, R., et al. (2016). The influences of drought and land-cover conversion on inter-annual variation of NPP in the Three-North shelterbelt program zone of China based on MODIS data. *PLoS One* 11 (6), e0158173. doi:10.1371/journal.pone.0158173

Peng, J., Dan, L., Ying, K., Yang, S., Tang, X., and Yang, F. (2021). China's interannual variability of net primary production is dominated by the central China region. *J. Geophys. Res. Atmos.* 126 (4), e2020JD033362. doi:10.1029/2020JD033362

Peng, S., Chen, A., Xu, L., Cao, C., Fang, J., Myneni, R. B., et al. (2011). Recent change of vegetation growth trend in China. *Environ. Res. Lett.* 6 (4), 044027. doi:10.1088/1748-9326/6/4/044027

Piao, S., Ciais, P., Huang, Y., Shen, Z., Peng, S., Li, J., et al. (2010). The impacts of climate change on water resources and agriculture in China. *Nature* 467 (7311), 43–51. doi:10.1038/nature09364

Piao, S., Ciais, P., Lomas, M., Beer, C., Liu, H., Fang, J., et al. (2011). Contribution of climate change and rising CO2 to terrestrial carbon balance in East asia: A multi-model analysis. *Glob. Planet. Change* 75 (3-4), 133–142. doi:10.1016/j.gloplacha.2010.10.014

Qi, X., Jia, J., Liu, H., and Lin, Z. (2019). Relative importance of climate change and human activities for vegetation changes on China's silk road economic belt over multiple timescales. *Catena* 180, 224–237. doi:10.1016/j.catena.2019.04.027

Qiu, C., Hu, J., Yang, F., Liu, F., and Li, X. (2018). Human pressures on natural reserves in yunnan province and management implications. *Sci. Rep.* 8 (1), 3260. doi:10.1038/s41598-018-21654-w

Roxburgh, S. H., Berry, S. L., Buckley, T. N., Barnes, B., and Roderick, M. L. (2005). What is NPP? Inconsistent accounting of respiratory fluxes in the definition of net primary production. *Funct. Ecol.* 19 (3), 378–382. doi:10.1111/j.1365-2435.2005.00983.x

Running, S. W., Nemani, R. R., Heinsch, F. A., Zhao, M., Reeves, M., and Hashimoto, H. (2004). A continuous satellite-derived measure of global terrestrial primary production. *Bioscience* 54 (6), 547–560. doi:10.1641/0006-3568(2004)054[0547:Acsmog]2.0.Co;2

Sha, Z., Bai, Y., Lan, H., Liu, X., Li, R., and Xie, Y. (2020). Can more carbon be captured by grasslands? A case study of inner Mongolia, China. *Sci. Total Environ.* 723, 138085. doi:10.1016/j.scitotenv.2020.138085

Sharma, S., Joshi, P. K., and Furst, C. (2022). Unravelling net primary productivity dynamics under urbanization and climate change in the Western Himalaya. *Ecol. Indic.* 144, 109508. doi:10.1016/j.ecolind.2022.109508

Shen, X., Liu, B., Jiang, M., and Lu, X. (2020). Marshland loss warms local land surface temperature in China. *Geophys. Res. Lett.* 47 (6), e2020GL087648. doi:10.1029/2020GL087648

Shen, X., Liu, Y., Zhang, J., Wang, Y., Ma, R., Liu, B., et al. (2022). Asymmetric impacts of diurnal warming on vegetation carbon sequestration of marshes in the Qinghai Tibet Plateau. *Glob. Biogeochem. Cycles* 36 (7), e2022GB007396. doi:10.1029/2022GB007396

Shi, X., Shi, M., Zhang, N., Wu, M., Ding, H., Li, Y., et al. (2022). Effects of climate change and human activities on gross primary productivity in the Heihe River Basin, China. *Environ. Sci. Pollut. Res.* 30, 4230–4244. doi:10.1007/s11356-022-22505-y

Song, Y., Achberger, C., and Linderholm, H. W. (2011). Rain-season trends in precipitation and their effect in different climate regions of China during 1961-2008. *Environ. Res. Lett.* 6 (3), 034025–034346. doi:10.1088/1748-9326/6/3/034025

Song, Y., and Ma, M. (2011). A statistical analysis of the relationship between climatic factors and the Normalized Difference Vegetation Index in China. *Int. J. Remote Sens.* 32 (14), 3947–3965. doi:10.1080/01431161003801336

Su, B., Huang, J., Fischer, T., Wang, Y., Kundzewicz, Z. W., Zhai, J., et al. (2018). Drought losses in China might double between the 1.5 °C and 2.0 °C warming. *Proc. Natl. Acad. Sci. U. S. A.* 115 (42), 10600–10605. doi:10.1073/pnas.1802129115

Sun, R., Liu, C., and Zhu, Q. (2002). Dynamic change of net primary productivity and fractional vegetation cover in the Yellow River Basin using multi-temporal AVHRR NDVI Data. *J. Geog. Sci.* 12 (1), 29–34. doi:10.1007/bf02837424

Sun, Y., Yang, Y., Zhang, L., and Wang, Z. (2015). The relative roles of climate variations and human activities in vegetation change in North China. *Phys. Chem. Earth* 87-88, 67–78. doi:10.1016/j.pce.2015.09.017

Tang, L., Gao, L., and Shi, L. (2015). Sustainable management and protection of ecosystems in shangri-La county, yunnan province, China: Introduction. *Int. J. Sustain. Dev. World Ecol.* 22 (2), 99–102. doi:10.1080/13504509.2014.943331

Tang, X., Xiao, J., Ma, M., Yang, H., Li, X., Ding, Z., et al. (2022). Satellite evidence for China's leading role in restoring vegetation productivity over global karst ecosystems. *For. Ecol. Manage.* 507, 120000. doi:10.1016/j.foreco.2021.120000

Tian, J., Wang, B., Zhang, C., Li, W., and Wang, S. (2020). Mechanism of regional land use transition in underdeveloped areas of China: A case study of northeast China. *Land Use Policy* 94, 104538. doi:10.1016/j.landusepol.2020.104538

Turner, M. G., and Carpenter, S. R. (2017). Ecosystem modeling for the 21st century. *Ecosystems* 20 (2), 211–214. doi:10.1007/s10021-016-0076-x

van der Molen, M. K., Dolman, A. J., Ciais, P., Eglin, T., Gobron, N., Law, B. E., et al. (2011). Drought and ecosystem carbon cycling. *Agric. For. Meteorol.* 151 (7), 765–773. doi:10.1016/j.agrformet.2011.01.018

Wang, B., Gao, P., Niu, X., and Sun, J. (2017). Policy-driven China's Grain to green program: Implications for ecosystem services. *Ecosyst. Serv.* 27, 38–47. doi:10.1016/j.ecoser.2017.07.014

Wang, J., Dong, J., Yi, Y., Lu, G., Oyler, J., Smith, W. K., et al. (2017). Decreasing net primary production due to drought and slight decreases in solar radiation in China from 2000 to 2012. *J. Geophys. Res. Biogeo.* 122 (1), 261–278. doi:10.1002/2016JG003417

Wang, J., Price, K. P., and Rich, P. M. (2001). Spatial patterns of NDVI in response to precipitation and temperature in the central Great Plains. *Int. J. Remote Sens.* 22 (18), 3827–3844. doi:10.1080/01431160010007033

Wang, M., Ding, Z., Wu, C., Song, L., Ma, M., Yu, P., et al. (2021a). Divergent responses of ecosystem water-use efficiency to extreme seasonal droughts in Southwest China. *Sci. Total Environ.* 760, 143427. doi:10.1016/j.scitotenv.2020.143427

Wang, M., Wang, S., Zhao, J., Ju, W., and Hao, Z. (2021b). Global positive gross primary productivity extremes and climate contributions during 1982-2016. *Sci. Total Environ.* 774, 145703. doi:10.1016/j.scitotenv.2021.145703

Wang, S., Zhang, B., Yang, Q., Chen, G., Yang, B., Lu, L., et al. (2017). Responses of net primary productivity to phenological dynamics in the Tibetan Plateau, China. *Agric. For. Meteorol.* 232, 235–246. doi:10.1016/j.agrformet.2016.08.020

Wang, S., Zhang, Y., Ju, W., Chen, J. M., Ciais, P., Cescatti, A., et al. (2020). Recent global decline of CO2 fertilization effects on vegetation photosynthesis. *Science* 370 (6522), 1295–1300. doi:10.1126/science.abb7772

Wen, Y., Liu, X., Bai, Y., Sun, Y., Yang, J., Lin, K., et al. (2019). Determining the impacts of climate change and urban expansion on terrestrial net primary production in China. *J. Environ. Manage.* 240, 75–83. doi:10.1016/j.jenvman.2019.03.071

Wu, G., Cheng, Z., Alatalo, J. M., Zhao, J., and Liu, Y. (2021). Climate warming consistently reduces grassland ecosystem productivity. *Earths Future* 9 (6). doi:10.1029/2020EF001837

Wu, H., Zhang, J., Bao, Z., Wang, G., Wang, W., Yang, Y., et al. (2022). The impacts of natural and anthropogenic factors on vegetation change in the Yellow-Huai-Hai River Basin. *Front. Earth Sci.* 10, 959403. doi:10.3389/feart.2022.959403

Wu, N., Liu, A., Ye, R., Yu, D., Du, W., Chaolumeng, Q., et al. (2021). Quantitative analysis of relative impacts of climate change and human activities on Xilingol grassland in recent 40 years. *Glob. Ecol. Conserv.* 32, e01884. doi:10.1016/j.gecco.2021.e01884

Wu, S., Zhou, S., Chen, D., Wei, Z., Dai, L., and Li, X. (2014). Determining the contributions of urbanisation and climate change to NPP variations over the last decade in the Yangtze River Delta, China. *Sci. Total Environ.* 472, 397–406. doi:10.1016/j.scitotenv.2013.10.128

Xiao, J., and Zhuang, Q. (2007). Drought effects on large fire activity in Canadian and Alaskan forests. *Environ. Res. Lett.* 2 (4), 044003. doi:10.1088/1748-9326/2/4/044003

Xiong, Q., Pan, K., Zhang, L., Wang, Y., Li, W., He, X., et al. (2016). Warming and nitrogen deposition are interactive in shaping surface soil microbial communities near the alpine timberline zone on the eastern Qinghai-Tibet Plateau, southwestern China. *Appl. Soil Ecol.* 101, 72–83. doi:10.1016/j.apsoil.2016.01.011

Xiong, Q., Xiao, Y., Liang, P., Li, L., Zhang, L., Li, T., et al. (2021). Trends in climate change and human interventions indicate grassland productivity on the Qinghai-Tibetan Plateau from 1980 to 2015. *Ecol. Indic.* 129, 108010. doi:10.1016/j.ecolind.2021.108010

Xu, H., Wang, X., and Zhang, X. (2016). Alpine grasslands response to climatic factors and anthropogenic activities on the Tibetan Plateau from 2000 to 2012. *Ecol. Eng.* 92, 251–259. doi:10.1016/j.ecoleng.2016.04.005

Xu, J., Yin, R., Li, Z., and Liu, C. (2006). China's ecological rehabilitation: Unprecedented efforts, dramatic impacts, and requisite policies. *Ecol. Econ.* 57 (4), 595–607. doi:10.1016/j.ecolecon.2005.05.008

Xu, X., Jiang, H., Guan, M., Wang, L., Huang, Y., Jiang, Y., et al. (2020). Vegetation responses to extreme climatic indices in coastal China from 1986 to 2015. *Sci. Total Environ.* 744, 140784. doi:10.1016/j.scitotenv.2020.140784

Yan, M., Xue, M., Zhang, L., Tian, X., Chen, B., and Dong, Y. (2021). A decade's change in vegetation productivity and its response to climate change over northeast China. *Plants* 10 (5), 821. doi:10.3390/plants10050821

Yan, Y., Liu, X., Wen, Y., and Ou, J. (2019). Quantitative analysis of the contributions of climatic and human factors to grassland productivity in northern China. *Ecol. Indic.* 103, 542–553. doi:10.1016/j.ecolind.2019.04.020

Yang, H., Mu, S., and Li, J. (2014). Effects of ecological restoration projects on land use and land cover change and its influences on territorial NPP in Xinjiang, China. *Catena* 115, 85–95. doi:10.1016/j.catena.2013.11.020

Yang, H., Zhong, X., Deng, S., and Xu, H. (2021). Assessment of the impact of LUCC on NPP and its influencing factors in the Yangtze River basin, China. *Catena* 206, 105542. doi:10.1016/j.catena.2021.105542

Yang, J., Zhang, X., Luo, Z., and Yu, X. (2017). Nonlinear variations of net primary productivity and its relationship with climate and vegetation phenology, China. *Forests* 8 (10), 361. doi:10.3390/f8100361

Yang, Y., Guan, H., Shen, M., Liang, W., and Jiang, L. (2015). Changes in autumn vegetation dormancy onset date and the climate controls across temperate ecosystems in China from 1982 to 2010. *Glob. Change Biol.* 21 (2), 652–665. doi:10.1111/gcb.12778

Yin, L., Dai, E., Zheng, D., Wang, Y., Ma, L., and Tong, M. (2020). What drives the vegetation dynamics in the Hengduan Mountain region, southwest China: Climate change or human activity? *Ecol. Indic.* 112, 106013. doi:10.1016/j.ecolind.2019.106013

Yin, Y., Deng, H., and Ma, D. (2022). Complex effects of moisture conditions and temperature enhanced vegetation growth in the Arid/humid transition zone in Northern China. *Sci. Total Environ.* 805, 150152. doi:10.1016/j.scitotenv.2021.150152

Zeng, B., and Yang, T. (2008). Impacts of climate warming on vegetation in Qaidam Area from 1990 to 2003. *Environ. Monit. Assess.* 144 (1-3), 403–417. doi:10.1007/s10661-007-0003-x

Zhang, C., Wang, X., Li, J., and Hua, T. (2011). Roles of climate changes and human interventions in land degradation: A case study by net primary productivity analysis in China's shiyanghe basin. *Environ. Earth Sci.* 64 (8), 2183–2193. doi:10.1007/s12665-011-1046-4

Zhang, X., Moran, M. S., Zhao, X., Liu, S., Zhou, T., Ponce-Campos, G. E., et al. (2014). Impact of prolonged drought on rainfall use efficiency using MODIS data across China in the early 21st century. *Remote Sens. Environ.* 150, 188–197. doi:10.1016/j.rse.2014.05.003

Zhao, F., Xu, B., Yang, X., Xia, L., Jin, Y., Li, J., et al. (2019). Modelling and analysis of net primary productivity and its response mechanism to climate factors in temperate grassland, northern China. *Int. J. Remote Sens.* 40 (5-6), 2259–2277. doi:10.1080/01431161.2018.1516322

Zhao, L., Dai, A., and Dong, B. (2018). Changes in global vegetation activity and its driving factors during 1982-2013. *Agric. For. Meteorol.* 249, 198–209. doi:10.1016/j.agrformet.2017.11.013

Zhao, M., Heinsch, F. A., Nemani, R. R., and Running, S. W. (2005). Improvements of the MODIS terrestrial gross and net primary production global data set. *Remote Sens. Environ.* 95 (2), 164–176. doi:10.1016/j.rse.2004.12.011

Zhao, M., and Running, S. W. (2010). Drought-Induced reduction in global terrestrial net primary production from 2000 through 2009. *Science* 329 (5994), 940–943. doi:10.1126/science.1192666

Zhou, B., Liao, Z., Chen, S., Jia, H., Zhu, J., and Fei, X. (2022). Net primary productivity of forest ecosystems in the southwest karst region from the perspective of carbon neutralization. *Forests* 13 (9), 1367. doi:10.3390/f13091367

Zhou, W., Gang, C., Zhou, F., Li, J., Dong, X., and Zhao, C. (2015). Quantitative assessment of the individual contribution of climate and human factors to desertification in northwest China using net primary productivity as an indicator. *Ecol. Indic.* 48, 560–569. doi:10.1016/j.ecolind.2014.08.043

Zhou, X., Fei, S., Sherry, R., and Luo, Y. (2012). Root biomass dynamics under experimental warming and doubled precipitation in a tallgrass prairie. *Ecosystems* 15 (4), 542–554. doi:10.1007/s10021-012-9525-3